ELSEVIER

Contents lists available at ScienceDirect

Developments in the Built Environment

journal homepage: www.sciencedirect.com/journal/developments-in-the-built-environment





Properties of mortars containing crumb rubber and glass powder

Viviana Letelier^{a,*}, Marión Bustamante^b, Bruno Olave^a, Carola Martínez^a, José Marcos Ortega^c

- ^a Department of Civil Engineering, Universidad de La Frontera, Temuco, 4780000, Chile
- b Doctoral Program in Engineering at the MacroFacultad de Ingeniería UFRO-UBB-UTAL, Chile
- c Departamento de Ingeniería Civil, Universidad de Alicante, Alacant, 03080, Spain

ARTICLE INFO

Keywords: Crumb rubber Glass powder Mortar

ABSTRACT

This study presents an alternative for the combined revalorization of two wastes with high volumes of generation, such as end-of-life tyres and glass. The experimental grid considered the analysis of the joint use of crumb rubber and glass powder in mortars. Crumb rubber is analysed as a sand replacement at 10% and 15% percentages, while glass powder is'. analysed as a 10% replacement for cement, considering the effect of two maximum size particles (38 μm and 45 μm). The results obtained show a decrease in the mechanical strength of the mortars, mainly associated with the use of crumb rubber, which increases with the increase in the percentage of crumb rubber used. However, a synergistic effect of the joint use of crumb rubber with glass powder was observed, which allowed the improvement of not only the thermal properties of the series but also those of water absorption, porosity and capillarity.

1. Introduction

Worldwide, the constant development of construction has led to a high demand for building materials, and at the same time, a shortage in different locations of the raw materials required for these materials. For this reason, concern for the environment and the conscientious use of natural resources are the focus of several areas at the industrial level. Specifically, the construction industry is responsible for high percentages of carbon dioxide (CO₂) emissions and natural resource extraction (OECD, 2019). As a result, various strategies are being developed to mitigate the adverse effects that the industry is generating. These strategies include actions carried out for the increase of the circular economy in construction, which aim to reduce or eliminate solutions based on linear models of use and disposal, which imply a high consumption of natural resources (Hossain et al., 2020). Among these actions is the use of secondary materials from waste or debris (Letelier et al., 2019a).

A secondary material used within the construction area in various materials has been rubber tyre waste. This waste generates worldwide concern due to the high volumes generated annually and the environmental damage caused by the most common tyre disposal practices. From the available data it is considered that about 1.5 billion tyres are discarded annually across the globe (XU et al., 2020). The increase in tyre waste has become a major environmental problem, called "black pollution", since a common practice is to leave this waste in landfills or

unauthorised sites and the easiest and most economical method to dispose of tyres is to burn them.

There are currently several innovative techniques for recycling large volumes of scrap tyres. Depending on their crushing process and particle size, they can be used as an addition to or replacement for fine and coarse aggregates, and replaced as fibre, crumb or powder. Some options to reuse this waste are within cementitious materials, such as concrete or mortars, where crumb rubber (CR) is used as a partial or total replacement for natural aggregates (NA), allowing, among other things, a reduction in the demand for extraction of natural raw materials (XU et al., 2020). The main disadvantage of the use of CR in these materials is the weak interface that is generated between the CR particles and the cement paste, reducing its mechanical properties, but losses can be controlled by limiting its use percentages (Akhtar and Sarmah, 2018). However, an improvement in the physical and durability properties of the mixtures, such as corrosion resistance, acoustic and thermal insulation, has been demonstrated (Youssf et al., 2015; Zhu et al., 2019).

On the other hand, high volumes of glass are currently landfilled. Globally, glass recycling rates vary depending on the country being analysed. European Union countries have the highest recycling percentages in the world, with an average of 73%, while other countries have much lower values, such as the United States (34%) and Singapore (20%) (Heriyanto and Sahajwalla, 2018). In the case of Chile, available data show that the recycling rate in 2020 was 27% (Kyklos, 2020).

E-mail address: viviana.letelier@ufrontera.cl (V. Letelier).

^{*} Corresponding author.

The revalorization of glass within the construction industry is an attractive option, due to the industry's capacity to valorise a high percentage of this waste and the low quality conditions required. An effective alternative among construction materials is the use of glass powder (GP) as a cement replacement. The negative effects caused by the alkali-silica reaction caused by the use of glass do not occur when it is used as a cement substitute due to its pozzolanic properties. Chen et al. (2002) analysed the incorporation of a percentage of GP in cement production, concluding that cement produced with the addition of GP shows no chemical or physical differences with respect to cement produced without the addition of glass. In turn, studies by Ortega et al. (2018) reveal that the development of microstructure and serviceability properties is slower for mortars with GP than for control mortars due to the delay in pozzolanic reactions of GP compared to clinker hydration. The addition of GP by up to 20%, however, did not result in a loss of durability or medium-to long-term mechanical properties compared to control mortars (Ortega et al., 2018).

As a proposal to increase the environmental benefits generated by the use of secondary materials, studies have been conducted that incorporate two or more wastes to prepare cement-based materials. Despite this, there is still little or no literature on the combined use of crumb rubber and glass powder. Therefore, this study focuses mainly on the analysis and effect of incorporating these two wastes separately and combined in mortars, evaluating the possible synergies that may occur between the both wastes. The replacement of natural fine aggregates (NFA) by CR and the replacement of cement by GP will be analysed.

2. Materials and methods

2.1. Materials

2.1.1. Portland cement

High strength cement formulated with clinker, pozzolan and gypsum, classified as type IP (Portland-pozzolanic) according to ASTM C595/C595M - 16 (ASTM C595/C595M - 16, 2016), was used in this study. According to its technical data sheet, its initial and final setting time is 90 and 125 min, respectively. In addition, its Blaine specific surface area is 5000 $\rm cm^2/g$ and its specific weight is 3.00 g/cm². It has a SO3 content of 3.5%. Its compressive and tensile strengths at 7 days are 420 kg/cm² and 65 kg/cm², increasing to 500 kg/cm² and 75 kg/cm² at 28 days, respectively. Table 1 shows its chemical analysis.

2.1.2. Aggregates

The natural aggregate used corresponds to fine quartz sand obtained locally, washed and dried at 100 $^{\circ}\text{C}$ for 24 h and then sieved through meshes from No. 16 (1.18 mm) to No. 200 (0.075 mm). Table 2 shows the physical properties of this material, while Fig. 1 presents the particle size distribution used.

2.1.3. Waste glass

Glass powder (GP) was incorporated as waste to be used as a 10% cement replacement. The glass used was obtained from locally collected clear bottles, which were washed and their labels removed. After being dried, they were crushed and sieved until reaching mesh sizes No. 325

Table 1Chemical properties of cement and glass powder.

Composition	Cement (%)	GP (%)
SiO_2	38.06	64.32
Al_2O_3	8.88	2.90
CaO	40.92	18.18
Fe_2O_3	2.83	-
SO_3	2.33	-
MgO	1.59	-
Na ₂ O	1.75	13.03
K ₂ O	1.62	1.53

Table 2 Physical properties of the aggregates.

Aggregate type	Specific gravity (g/cm ³)	Absorption (%)	
Natural fine aggregate	2.6	0.8	
Crumb rubber	1.06	-	

(0.045 mm) and No. 400 (0.038 mm). To obtain the mineralogical composition of the crystalline phases of the GP, an X-ray diffraction analysis (XRD) was performed (Fig. 2). From this analysis it is not possible to identify peaks attributed to any crystallized compound, with the exception of a wide diffraction halo between 20° and 30°, which is attributed to the vitreous phase, characteristic of amorphous structures, similar to that obtained in a previous study by Kim et al. (2015). In addition, Fig. 3 shows the EDS (energy dispersive spectroscopy) of the GP used, which agrees with the data presented in Table 1. When making a cement replacement, it is important that the sum of the Si + Al + Cacomponents be greater than 75%, which it is possible to observe in the figure representing the principal components of the GP. Fig. 4a shows the shape of the glass particles, which in this case are angular and flattened, as well as an idea of their particle size distribution. These aspects are important to explain some behaviours such as consistency, or the filler effect that contributes to the properties of the mortar. Fig. 5 shows the particle size obtained from the laser diffraction analysis, from which it is observed that, despite the low average values of the two samples, the particle size of GP-38 μm is more concentrated in the fine fractions than those of GP-45 µm.

2.1.4. Tyre rubber waste

Replacement percentages of 10% and 15% crumb rubber (CR) by volume of NFA were used. This waste was supplied by a local tyre company, it was shredded, washed and the steel fibres were extracted. The CR was then sieved through 1.18, 0.6, 0.3 and 0.15 mm meshes. Table 2 shows some physical properties of this waste. In addition, Fig. 4b presents the SEM analysis of the CR, which shows a smooth surface to the naked eye.

2.2. Mix proportions

The mix proportions of all series are given in Table 3. In order to study the influence of each waste on the mixture, 9 series were carried out, considering a control series (C00) to compare the results obtained. All the series were based on the control series, designed with a cement: sand ratio of 1:3. The water used corresponds to that required to maintain a consistency of 210 \pm 5 mm.

2.3. Testing methods

2.3.1. Consistency

To ensure an adequate workability and the comparison between mortars, consistency values were set in the spreading range of 210 ± 5 mm according to NCh2256/1.Of2001 (NCh2256/1.Of 2001, 2001) with a 100 mm internal diameter mini slump cone on a 250 mm flow table disc. The mould was first filled with the fresh mortar and then lifted vertically from the flow table to spread the mortar mixture on the disc. Subsequently, the flow table was agitated 15 times at a constant rate. After the mixture was stirred, two perpendicular diameter measurements of the mortar were taken. The final measurement was obtained from the average of 3 samples and a precision of 1 mm was considered.

2.3.2. Dry density

Dry density (ρ_d) was calculated according to UNE-EN 1015-10 (UNE-EN 1015-10, 2000). For this test, at 28 days of curing, 3 cylindrical samples (100 mm in diameter and 50 mm in height) were used. The test consisted of drying the samples in an oven at 105 °C for a minimum of 24 h, recording their dry weight (A). Subsequently, they

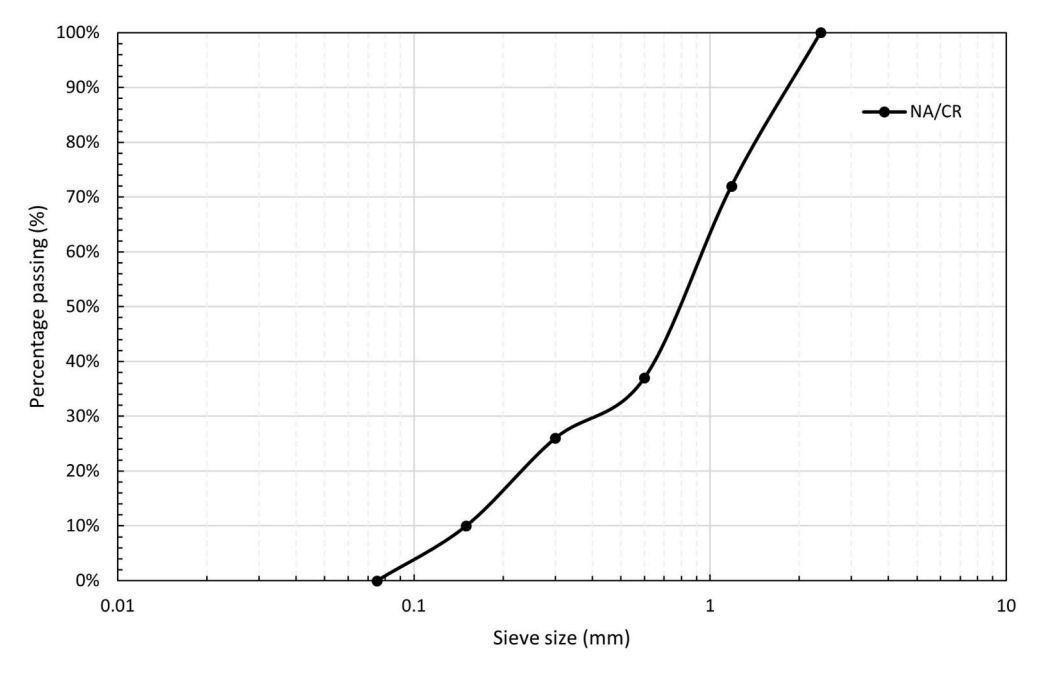


Fig. 1. Particle size distribution used for NA and CR.

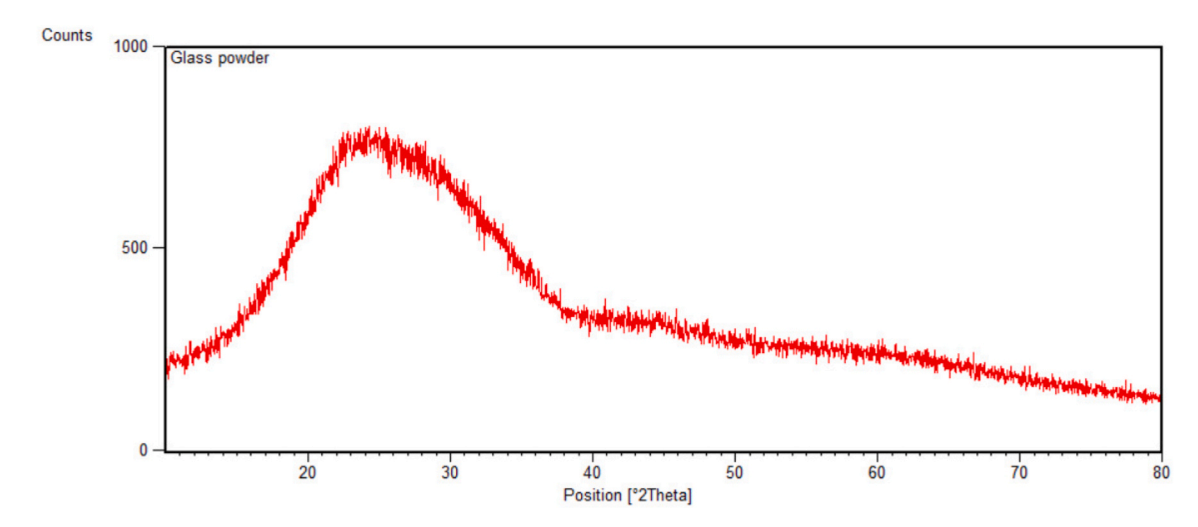


Fig. 2. XRD analysis of glass powder used.

were immersed in water for another 24 h and the weight of the sample suspended in water was measured, obtaining the submerged weight (C). Finally, the samples were surface dried to obtain the saturated weight (B). With the obtained data, the dry density value was calculated using Equation (1).

$$\rho_d = \frac{A}{B - C} \gamma \tag{1}$$

where γ is the water density in g/cm³.

2.3.3. Water absorption by immersion

From the results obtained for the dry density, the water absorption by immersion, Abs (%), was calculated according to UNE-EN 1015-18 (UNE-EN 1015-18, 2003), using the formula shown in Equation (2).

$$Abs(\%) = \frac{B - A}{A} \cdot 100 \tag{2}$$

2.3.4. Water-accessible porosity

The accessible porosity (AP) was calculated according to UNE-EN 1015-18 (UNE-EN 1015-18, 2003) based on the data collected for the dry density test using Equation (3).

$$P_a = \frac{B - A}{B - C} \cdot 100 \tag{3}$$

2.3.5. Capillary absorption test

The water absorption rate was determined according to ASTM C1585-13 (ASTM C1585-13, 2013). Three cylindrical samples (100 mm in diameter and 50 mm in height) were used to measure the mass increase due to water absorption as a function of time. For this purpose, the sample is waterproofed so that only a free surface remains in contact with the water so that it rises vertically. In the first measurement period, the initial water absorption rate (cm/s $^{1/2}$) was obtained from the slope between the data measured between 1 min and 6 h.

2.3.6. Ultrasonic pulse velocity (UPV) test

To verify the homogeneity of the mortar, the presence of voids or

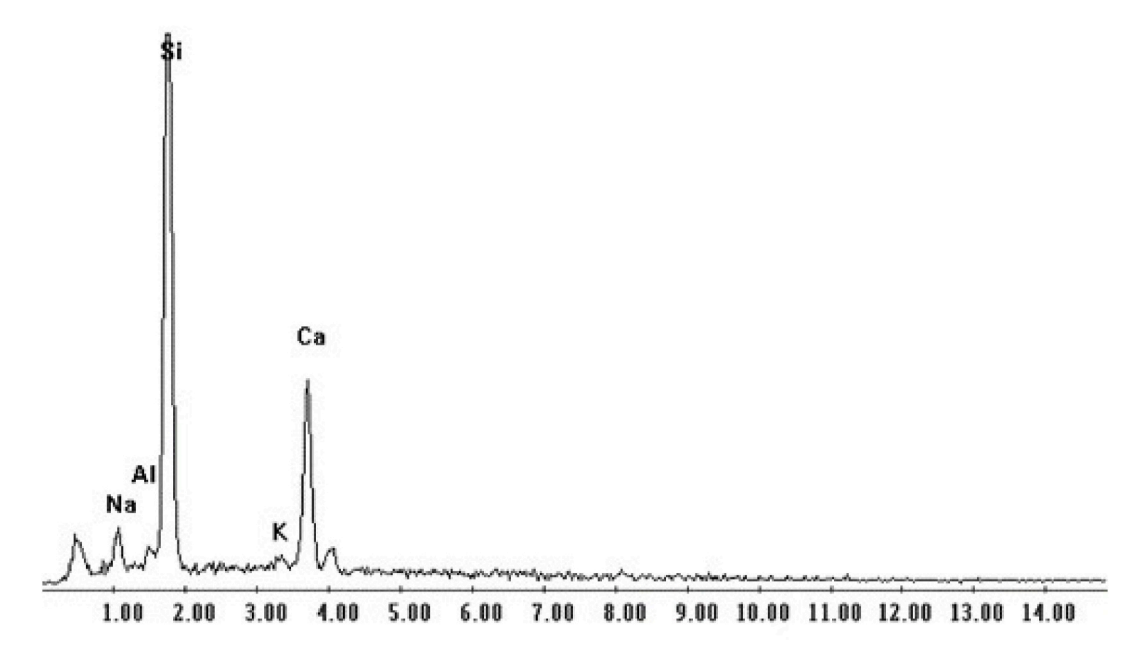


Fig. 3. EDS analysis of glass powder used.

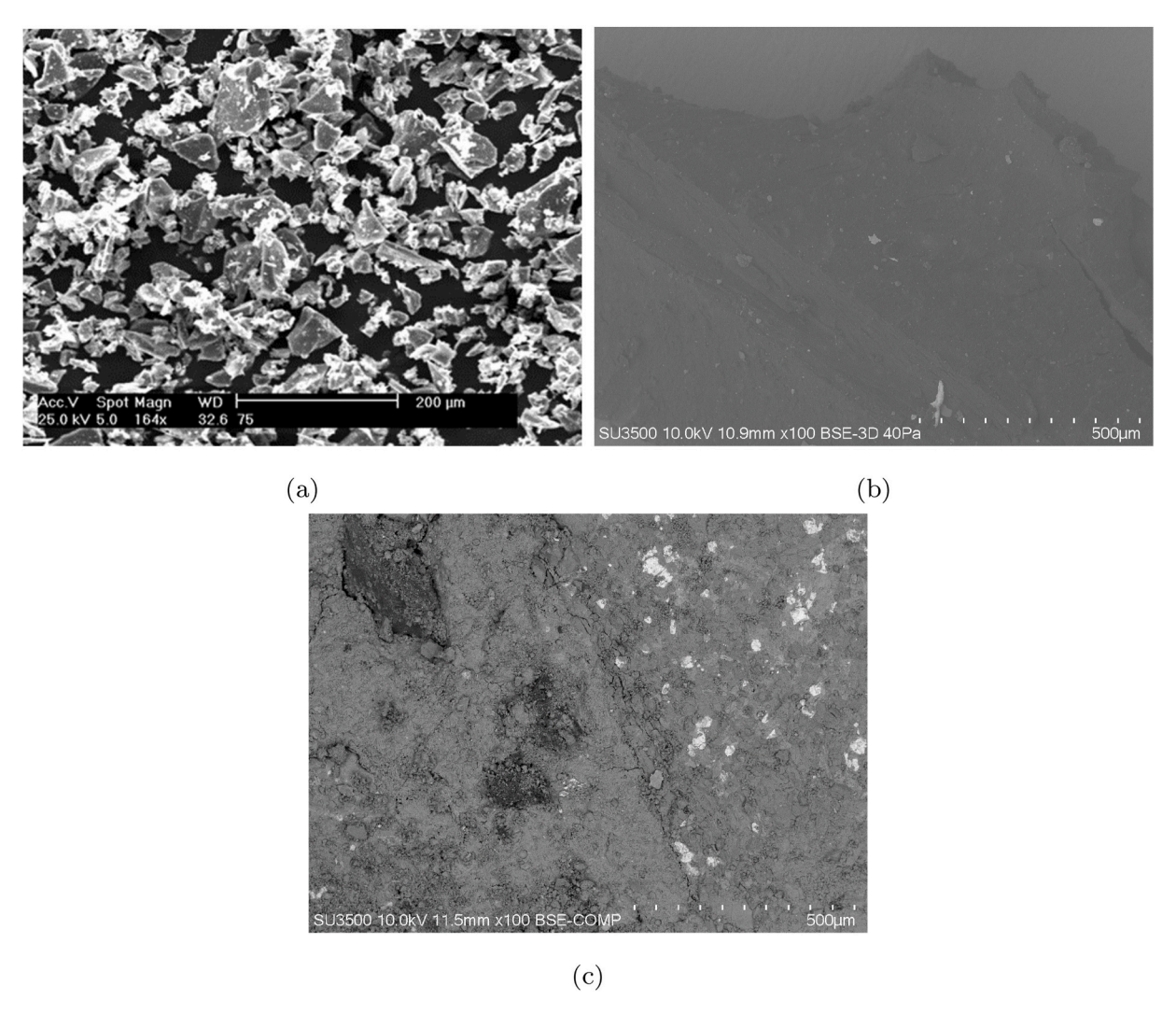


Fig. 4. SEM images of (a) Glass Powder, (b) Crumb Rubber, and (c) Cement matrix with addition of crumb rubber.

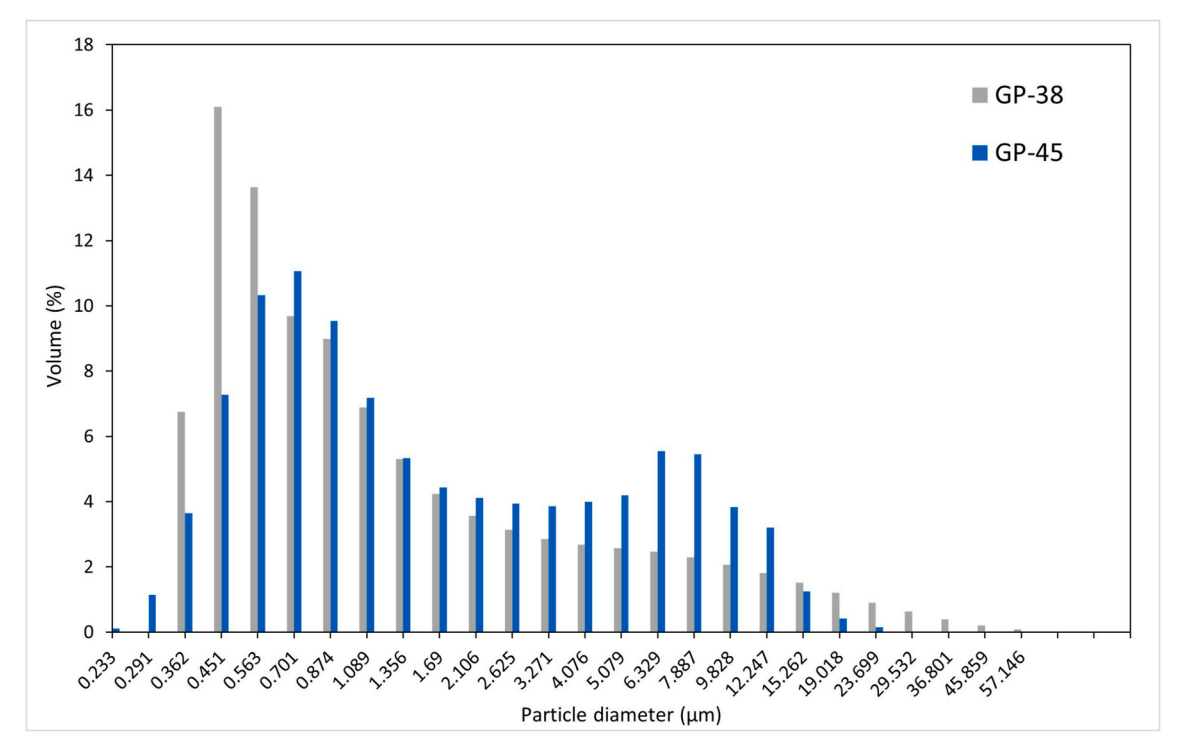


Fig. 5. Granulometry of the glass powder (38 and 45 μm).

Table 3
Mix proportions (g).

This proportions (g).									
Mix code	Water	Cement	w/b effective	GP (38 μm)	GP (45 μm)	Crumb rubber	Natural aggregate		
C00	288.00	450	0.64	0	0	0.00	1350.0		
CR10	300.86	450	0.67	0	0	55.47	1215.0		
CR15	313.71	450	0.70	0	0	83.20	1147.5		
GP38	288.00	405	0.64	45	0	0.00	1350.0		
GP45	288.00	405	0.64	0	45	0.00	1350.0		
CR10/GP38	306.00	405	0.68	45	0	55.47	1215.0		
CR10/GP45	306.00	405	0.68	0	45	55.47	1215.0		
CR15/GP38	324.00	405	0.72	45	0	83.20	1147.5		
CR15/GP45	324.00	405	0.72	0	45	83.20	1147.5		

cracks and possible changes over time, as well as to determine the physical and dynamic characteristics of the material, the ultrasonic pulse velocity method (UPV) was used. This test consists of determining the propagation velocity of a sound wave within the material by determining the time it takes for the wave to pass through a given thickness. Measurements were performed on 3 cylindrical samples (100 mm in diameter and 50 mm in height) according to ASTM C597-09 (ASTM C597-09, 2009) using a PULSONIC 58-E4900 instrument (CONTROLS). The time taken for the ultrasonic pulse to travel through the sample was measured to an accuracy of up to 0.1 μs , using 54 kHz transducers located at the centre of opposite faces of each sample.

2.3.7. Thermal conductivity

In order to determine the thermal conductivity of the mortars, non-destructive testing was carried out using the thermal needle probe procedure according to ASTM D5334-14 (ASTM D5334-14, 2014). For this purpose, a KD2 Pro equipment was used on cylindrical specimens 50 mm in diameter and 150 mm in height. The specimens were left to dry previously for 24 h at 70 °C, and then left at a room temperature of 20 °C for an additional 24 h prior to testing. As for the measurement, the heat generated by the needle inside the sample during a time t produces a temperature gradient, which is detected and recorded by the equipment. This temperature is calculated by Equation (4), and the thermal conductivity (γ) is determined by Equation (5) (Norambuena-Contreras

et al., 2018).

$$T = m_1 + m_2 \cdot t + m_3 \cdot \ln(t) \cdot Ec \tag{4}$$

where T is the recorded temperature; m_1 is the room temperature; m_2 is the rate of change of the background temperature; m_3 is the slope of a line relating the temperature increase to the logarithm of the temperature; and t is the test time.

$$\gamma = \frac{q}{4 \cdot \pi \cdot m_3} \cdot Ec \tag{5}$$

where the thermal conductivity γ is measured in W/mK; q is the heat generated by the needle sensor in W/m, where each value is determined as the average of 3 measurements.

2.3.8. Mechanical properties (compressive and flexural strength)

Compressive and flexural strength were determined according to UNE-EN 196-1 (UNE-EN 196-1, 1996). The series were tested at 7, 14 and 28 days of curing. At each opportunity, 3 RILEM prismatic specimens of 4 \times 4 \times 16 cm were tested for each series, from which the average value was obtained.

3. Results and discussion

3.1. Consistency

Table 3 shows the water required for each series to maintain the specified consistency. As can be seen, with respect to the control mortar, the addition of CR increases the water requirement as the percentage of addition increases. In the case of the addition of 10% and 15% of rubber, the increase of water is 4.5% and 8.9%, respectively. de Souza Kazmierczak et al. (de Souza Kazmierczak et al., 2020) consider that the laminar shape of the CR particles would cause a decrease in workability, which would explain the higher water consumption needed to maintain the workability. Mundo et al. (2020) consider that another factor influencing the increase in the water requirement is the hydrophobic character of CR particles.

On the other hand, when 10% GP is used, regardless of the particle size, no differences are observed with respect to the water required by the CM. According to Ramdani et al. (2019), the low water absorption of the glass powder could help to avoid changes in the required water. For their part, Letelier et al. (2019a) comment that the workability of the mortars is affected by the GP particle size, with a lower water requirement observed when GP particles were smaller than 38 $\mu m.$ xin Lu et al. (xin Lu et al., 2017) conclude that when the particle size is reduced, the consistency of the mortar increases to values even higher than those of the control mortar, probably because the thinner particles are able to reduce friction due to the irregular shape.

When both wastes are used together (CR and GP) there is an increase in the water required in percentages between 6.3% and 12.5%. These values are clearly affected by the use of rubber, but their values increase compared to the use of rubber alone, probably due to the irregular shape of the particles of both wastes and the difficult bonding of the rubber and glass particles in the fresh mixture.

3.2. Dry density

Fig. 6 shows the density of the series analysed at 28 days. As can be seen, when CR is used, compared to the control series, the density decreases noticeably as the rubber content increases in percentages of 8% and 12% for the 10% and 15% replacement, respectively. This decrease is mainly due to the lower density of the CR compared to the density of natural sand. On the other hand, the use of GP decreases the density of the series by only 1% with respect to CM, due to the lower density of the glass particles.

When both wastes are used together, a decrease in density varying between 9% and 11% with respect to the density of the CM is observed.

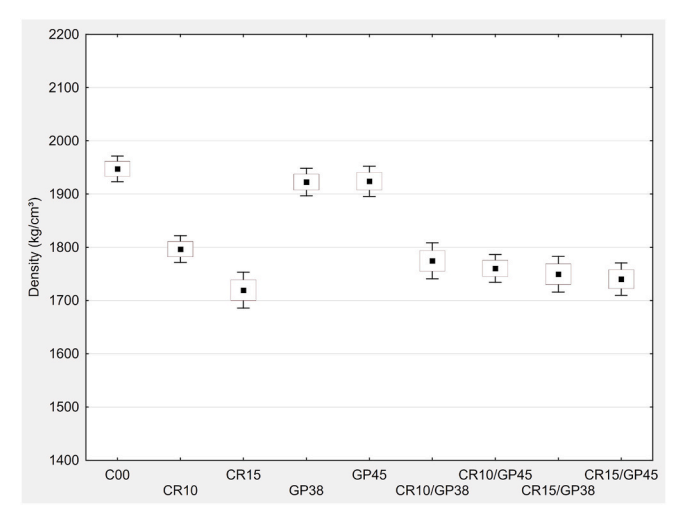


Fig. 6. Density at 28 days.

This decrease is mainly governed by the effect of the rubber particles.

3.3. Water absorption

Fig. 7 shows the water absorption of the series analysed. When CR is used, compared to the control series, water absorption increases as the rubber content increases in percentages of 6% and 24% for 10% and 15% replacement, respectively. This increase could be mainly due to the irregular shape of the rubber particles, as well as the greater amount of water required to maintain the consistency. In this way, the water that did not react with the cement particles is evaporated, generating voids that cause an increase in the water absorption (Wang et al., 2020).

From the results obtained at 28 days, when GP is used, an increase in water absorption is generated compared to CM, in percentages of 7% and 9% for the glass powder size of 38 μ m and 45 μ m, respectively. This increase is associated with an increase in porosity, which, according to several authors, is due to dilution effects (Mejdi et al., 2022; Nahi et al., 2020), meaning a reduction in the overall volume of cementitious materials (increasing the effective w/c ratio) and, consequently, a reduction in the formation amount of hydration products (Boukhelf et al., 2021; Du et al., 2021). The GP with nominal size of 38 μ m presents a slightly lower water absorption than the GP with a nominal size of 45 μ m, mainly due to the higher pore sealing capacity of the smaller size glass particles, generating a filler effect (Letelier et al., 2019a).

When both wastes are used, the water absorption percentages are considerably lower than when the wastes are used individually. Thus for 10% rubber replacements, the absorptions present differences with respect to the CM of 0% and 4% for the 38 μ m and 45 μ m sizes, respectively. On the other hand, when using 15% rubber, the absorptions present differences with respect to the CM of 2% and 6% for the sizes of 38 μ m and 45 μ m, respectively. The above reveals a synergistic effect of the use of both wastes, which allows sealing of the open pores (Ramdani et al., 2019).

3.4. Open porosity

According to Fig. 8, the incorporation of CR presented porosity values very close to the CM, with differences close to 0% and 9% when using 10% and 15% CR. These slight increases are due to the tendency of CR to repel water and attract air (Assaggaf et al., 2021), generating spaces or voids in the ITZ and weak bonds at the interface between the rubber and particles and the cement mixture (Moreno et al., 2020).

On the other hand, when replacing cement with GP, compared to CM, water porosity increases by 6% and 7% for 10% replacements of 38 μm and 45 μm particles, respectively. These increases have been

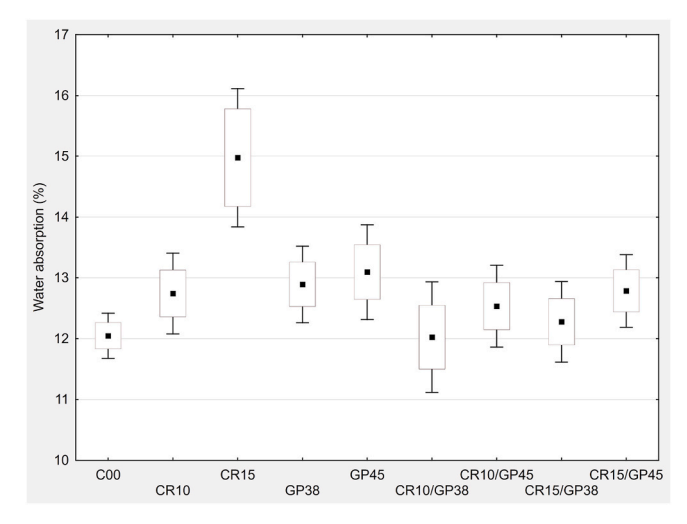


Fig. 7. Water absorption at 28 days.

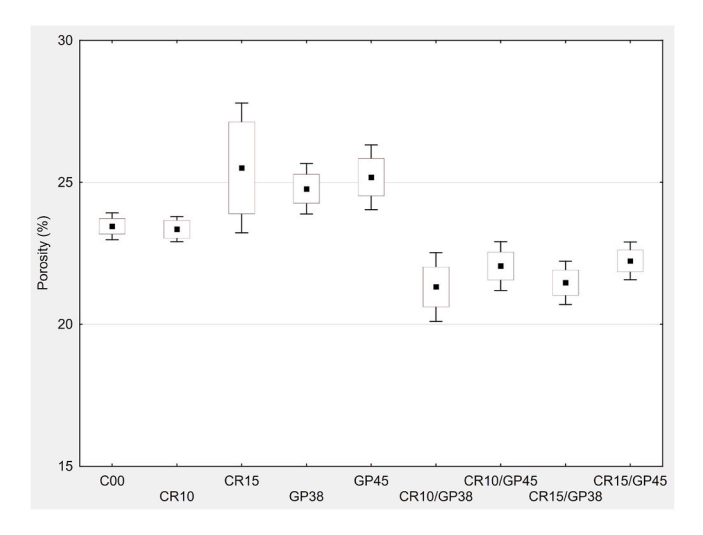


Fig. 8. Porosity at 28 days.

reported in several studies (Nahi et al., 2020; Du et al., 2021), which attribute the increase in porosity to the dilution effect when cement is replaced by GP, since there are fewer cement particles and more water in the matrix. Thus, when drying takes place, the water comes out and makes the mortar more porous. In turn, glass powder has a lower specific gravity than cement and the substitution by mass leads to less paste volume in the mortar.

When both wastes are used together, a decrease in porosity values with respect to CM is observed. When 10% CR is used, the porosity values are lower by 9% and 6% for GP sizes of 38 μm and 45 μm , respectively. In contrast, when 15% CR is used, the porosity values with respect to CM are lower by 9% and 5% for GP sizes of 38 μm and 45 μm , respectively. The above reveals a synergistic effect of the use of both wastes, which contributes to pore filling. These results could represent an opportunity to use this type of mortars in solutions that do not require high strength but impermeability of the material.

3.5. Capillarity

From the capillarity data available at 28 days (Fig. 9), it can be observed that when using 10% CR the capillarity values are higher by 3% with respect to those of the control series, and that with the increase of CR replacement to 15% the difference increases to 11%. These results can be explained by the higher porosity of the series with CR reported previously.

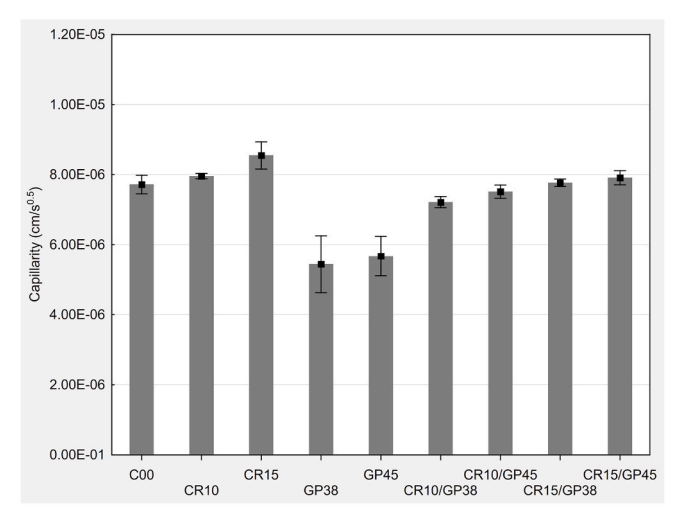


Fig. 9. Capillarity at 28 days.

When GP alone is used, considerable decreases in capillarity were observed with respect to CM. Thus, when 10% GP is used for GP sizes of 38 μm and 45 μm , the capillarity decreases by 29% and 26%, respectively, which may be related to the low absorption of GP.

When both wastes are used together, the series present capillarity values close to or lower than the CM. When 10% rubber is used, the capillarity values are lower by 7% and 3% for GP sizes of 38 μm and 45 μm , respectively. In contrast, when 15% CR is used, the capillarity values with respect to CM are higher by 1% and 3% for GP sizes of 38 μm and 45 μm , respectively. This reflects the benefit of the synergistic effect of both wastes, similar to what was observed in water absorption and porosity. Balasubramanian et al. (2021) studied the joint use of glass powder with electronic plastic. In analysing the various properties, they conclude that the use of both wastes performs better than the use of appliance plastic alone, which they attribute to the synergistic effect, which restored the pore filling and elasticity of the mixtures.

3.6. Ultrasonic pulse velocity

From Fig. 10, it is observed that when using CR the ultrasonic pulse velocity (UPV) decreases as the percentage of rubber replacement increases by percentages of 34% and 41% when using 10% and 15% CR, respectively. According to Assaggaf et al. (2021), the decrease in UPV values is due to the increase in acoustic vibration absorption due to the increase in porosity.

It can be observed that, as expected, as the rubber content in mortar increases, the pulse velocity decreases, and, therefore, the mortar strength decreases. This reduction is probably due to the relative slowing of the ultrasonic pulses when passing through cracks, voids and air or water filled defects caused by the addition of rubber aggregates. In addition, rubber aggregates have a higher sound isolation coefficient than mineral aggregates (Ramdani et al., 2019).

On the other hand, when GP alone is used, UPV values very close to the control series are observed, with losses of only 5% and 4% when 10% GP is used for GP sizes of 38 μm and 45 μm . According to several authors (Huynh et al., 2018; Letelier et al., 2019b), smaller particle sizes generate a filling effect, which allows the production of more compact matrices and denser structure.

When both wastes are used, the UPV values decrease in high proportions, mainly affected by the use of rubber. When 10% CR is used, with respect to the control series, the UPV values decrease by 34% and 35% for GP sizes of 38 μm and 45 μm . When 15% CR is used, the UPV values decrease by 36% and 37% for GP sizes of 38 μm and 45 μm .

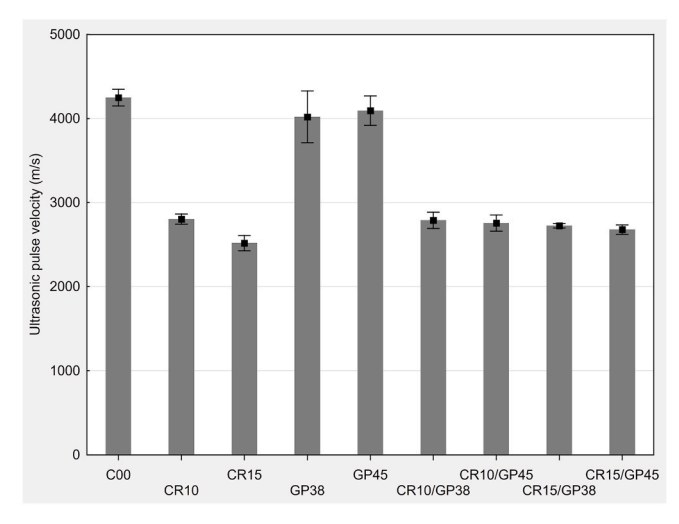


Fig. 10. Ultrasonic pulse velocity at 28 days.

3.7. Thermal conductivity

According to Fig. 11, the use of CR significantly improved the thermal performance of the samples. Compared to CM, replacement with 10% and 15% CR decreased the conductivity by an average of 21% and 29%, respectively. These data coincide with the results of several studies where it is observed that the replacement of natural aggregates with rubber decreases the thermal conductivity of concrete. This is due, on the one hand, to the air trapped in the mixture as a result of the poor adhesion of the cement mortar to the rubber surface (de Souza Kazmierczak et al., 2020; Marie, 2017), and on the other to the low thermal conductivity of rubber with respect to NA, which have values of 0.16 W/mK and 3.5 W/mK, respectively (Letelier et al., 2021).

When GP is used, the thermal conductivity values are slightly lower than the reference series, with decreases of 1% and 2% when using GP sizes of 38 μm and 45 μm . Boukhelf et al. (2021) consider that this decrease is related to the porosity increases of the series with GP. However, these decreases are slight due to the low percentages of GP used

When both wastes are used together, the thermal conductivity is clearly influenced by the use of CR. When 10% rubber is used, the thermal conductivity values are lower by 12% and 16% for GP sizes of 38 μm and 45 μm , respectively. In contrast, when 15% CR is used, the conductivity values with respect to CM are lower by 25% and 27% for GP sizes of 38 μm and 45 μm , respectively.

3.8. Compressive strength

Fig. 12 shows the behaviour of the compressive strength of the series under study at 7, 14 and 28 days. As can be seen, in all the series, the use of rubber particles significantly reduces the compressive strength. In the series where only rubber is replaced, the 28 day strength losses are 38% and 53% for CR replacements of 10% and 15%, respectively. According to Ren et al. (2022), the main reasons for the decrease in strength are (1) the hydrophobic nature of rubber, causing weak ITZ performance, (2) a lower modulus of elasticity, which induces high stress concentrations and crack propagation, and (3) non-uniform distribution attributed to its low density.

In the case of cement replacement by GP, it is possible to observe values much closer to the control series with differences at 28 days of 8% and 17% for GP replacements of 38 μ m and 45 μ m, respectively. It is observed that the strength of the series is affected by the GP particle size, with mortars with finer GP particles reaching higher strengths. According to Letelier et al. (2019a), this is mainly due to the combined effect of the physical and pozzolanic properties of GP particles smaller

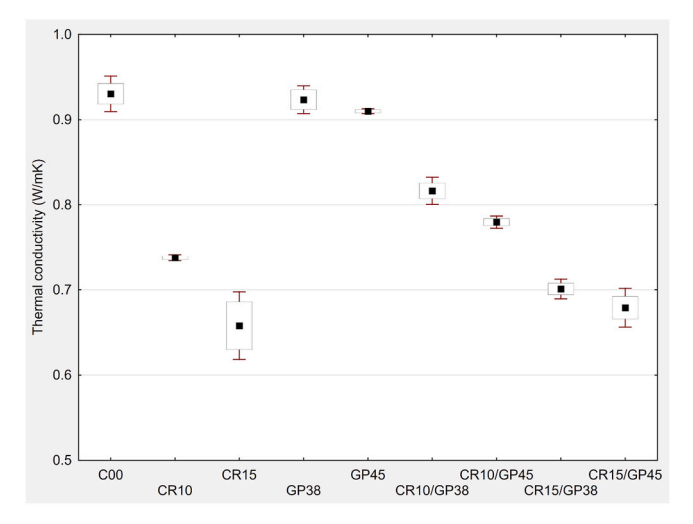


Fig. 11. Thermal conductivity at 28 days.

than 45 μ m. First, the finer GP particles have a filler effect, reducing the pore volume in the hardened matrix. On the other hand, the reaction between the amorphous GP compounds, such as alumina and silica, with portlandite produces silicate/aluminate hydrates similar to those produced as a result of cement hydration.

When both wastes are used simultaneously, a high influence of the use of CR is observed which causes a notable decrease in compressive strength. When 10% CR is used, the compressive strength values are lower by 48% and 50% for GP sizes of 38 μm and 45 μm , respectively. In contrast, when 15% CR is used, the strength values with respect to the CM are lower by 56% and 59% for GP sizes of 38 μm and 45 μm , respectively. In contrast with the synergistic effect discussed in the porosity and capillarity properties, in the case of mechanical properties, a clear negative effect of the use of CR is observed for the reasons discussed above.

3.9. Flexural strength

Fig. 13 shows the flexural strength behaviour of the series under study at 7, 14 and 28 days. Similar to the compressive behaviour, in all series the use of rubber particles significantly reduces the flexural strength. In the series where only rubber is replaced, the losses with respect to the control series at 28 days are 19% and 35% for 10% and 15% CR replacements, respectively. According to Alwesabi et al. (2020), the reduction in flexural strength is attributed to the weak bond between the mortar/aggregate and the rubber, which increases the stress concentration and accelerates crack propagation.

In the case of cement replacement by GP, the values obtained are closer to the control series, with differences at 28 days of 3% and 5% for GP replacements of 38 μm and 45 μm , respectively. Similar to the compressive strength, it is observed that the strength of the series is affected by the GP particle size, although this influence is less in the case of flexural strength.

When both wastes are used simultaneously, a behaviour influenced by the use of CR is observed. When 10% CR is used, the flexural strength values are lower by 27% and 30% for GP sizes of 38 μm and 45 μm , respectively. In contrast, when 15% CR is used, the flexural strength values with respect to CM are lower by 32% and 35% for GP sizes of 38 μm and 45 μm , respectively.

4. Conclusions

The main conclusions that can be drawn from the results analysed can be summarised as follows:

As reported in other investigations, the use of CR reduced the mechanical performance of the series in up to 53% and 35%, mainly associated with compressive and flexural strength, respectively. However, the combined use with GP improved the porosity, water absorption and capillarity of the specimens, obtaining values close to those of the control series, with an increase of 6% and 3% for water absorption and capillarity respectively, and a decrease of 5% for porosity. This result, along with the excellent thermal behaviour of the samples with CR that achieved values up to 29% lower than the CM, would confirm that the possible use of CR with GP can become an alternative for the revalorization of used tyre and glass waste in mortars with higher thermal performance, which do not require high mechanical strengths but greater impermeability.

On the other hand, although the decrease in the GP particle size improves the physical and mechanical behaviour of the series, mainly due to the greater filler effect of the particles, the influence is not significant enough to compensate for the energy required to obtain particles of a smaller size.

Declaration of competing interest

The authors declare that they have no known competing financial

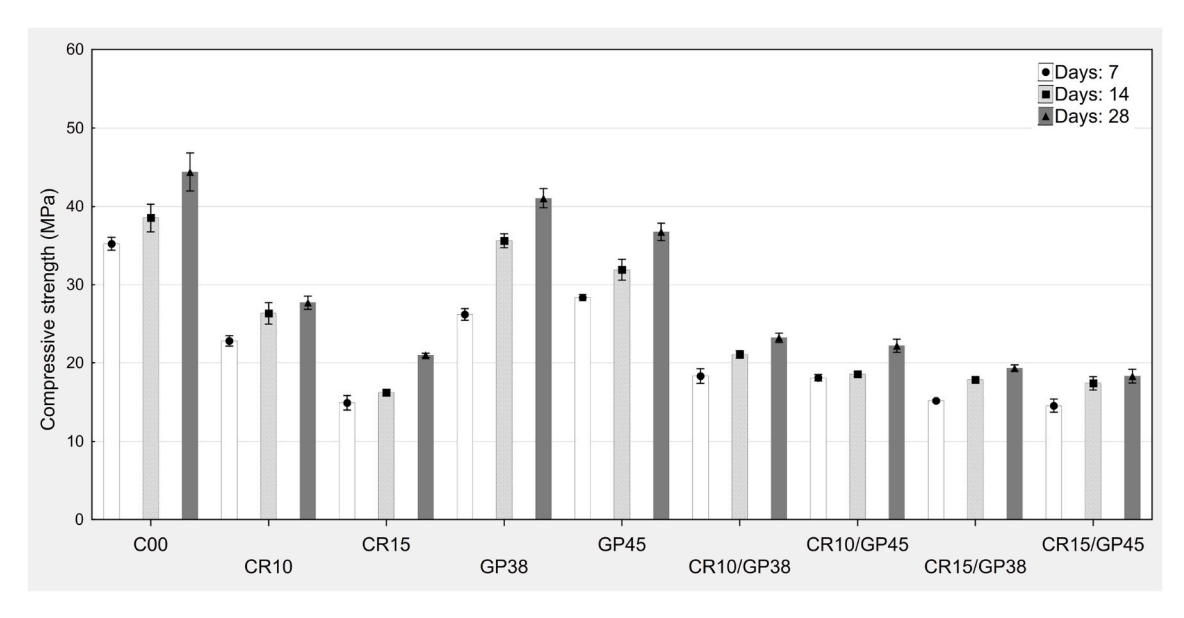


Fig. 12. Compressive strength a 7, 14 and 28 days.

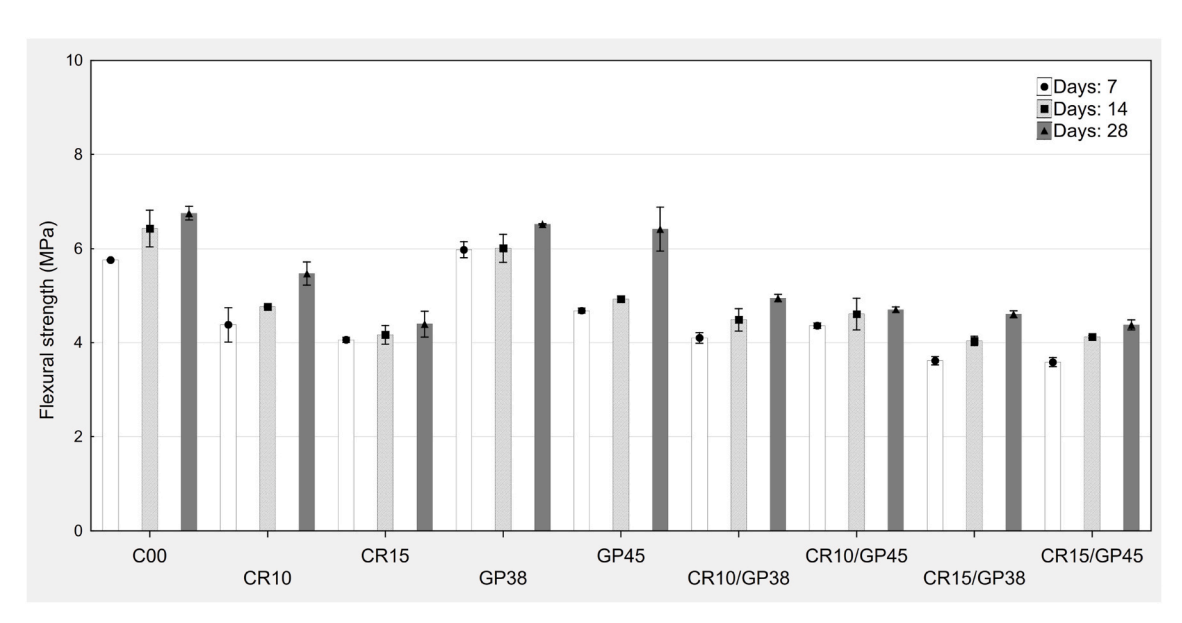


Fig. 13. Flexural strength at 7, 14 and 28 days.

interests or personal relationships that could have appeared to influence the work reported in this paper.

Acknowledgement

This work was supported by the Agencia Nacional de Investigación y Desarrollo de Chile (ANID) (Grant No. FONDECYT REGULAR 1211135). Additionally, the authors gratefully acknowledge the partial support from Universidad de La Frontera (Chile) (Projects DI18-0023 and DI19-0019).

References

Akhtar, A., Sarmah, A.K., 2018. Construction and demolition waste generation and properties of recycled aggregate concrete: a global perspective. J. Clean. Prod. 186, 262–281. https://doi.org/10.1016/j.jclepro.2018.03.085. URL: https://linkinghub.elsevier.com/retrieve/pii/S095965261830742X.

Alwesabi, E.A., Bakar, B.A., Alshaikh, I.M., Akil, H.M., 2020. Experimental investigation on mechanical properties of plain and rubberised concretes with steel–polypropylene hybrid fibre. Construct. Build. Mater. 233, 117194 https://doi.org/10.1016/j. $conbuild mat. 2019.117194. \ \ URL: \ https://linkinghub.elsevier.com/retrieve/pii/S0950061819326467.$

Assaggaf, R.A., Ali, M.R., Al-Dulaijan, S.U., Maslehuddin, M., 2021. Properties of concrete with untreated and treated crumb rubber – a review. J. Mater. Res. Technol. 11, 1753–1798. https://doi.org/10.1016/j.jmrt.2021.02.019. URL: https://linkinghub.elsevier.com/retrieve/pii/S2238785421001459.

ASTM C1585-13, 2013. Standard Test Method for Measurement of Rate of Absorption of Water by Hydraulic Cement Concretes. ASTM International, West Conshohocken,

ASTM C595/C595M-16, 2016. Standard specification for blended hydraulic cements. ASTM International, West Conshohocken, PA.

ASTM C597-09, 2009. Standard Test Method for Pulse Velocity through Concrete. ASTM International, West Conshohocken, PA.

ASTM D5334-14, 2014. Standard Test Method for Determination of Thermal Conductivity of Soil and Soft Rock by Thermal Needle Probe Procedure. ASTM International, West Conshohocken, PA.

Balasubramanian, B., Krishna, G.G., Saraswathy, V., Srinivasan, K., 2021. Experimental investigation on concrete partially replaced with waste glass powder and waste eplastic. Construct. Build. Mater. 278, 122400 https://doi.org/10.1016/j.conbuildmat.2021.122400. URL: https://linkinghub.elsevier.com/retrieve/pii/S0950061821001604.

Boukhelf, F., Cherif, R., Trabelsi, A., Belarbi, R., Bouiadjra, M.B., 2021. On the hygrothermal behavior of concrete containing glass powder and silica fume.

- J. Clean. Prod. 318, 128647 https://doi.org/10.1016/j.jclepro.2021.128647. URL: https://linkinghub.elsevier.com/retrieve/pii/S0959652621028493.
- Chen, G., Lee, H., Young, K.L., Yue, P.L., Wong, A., Tao, T., Choi, K.K., 2002. Glass recycling in cement production—an innovative approach. Waste Manag. 22, 747–753. https://doi.org/10.1016/S0956-053X(02)00047-8. URL: https://linkingh.ub.elsevier.com/retrieve/pii/S0956053X02000478.
- de Souza Kazmierczak, C., Schneider, S.D., Aguilera, O., Albert, C.C., Mancio, M., 2020. Rendering mortars with crumb rubber: mechanical strength, thermal and fire properties and durability behaviour. Construct. Build. Mater. 253, 119002 https://doi.org/10.1016/j.conbuildmat.2020.119002. URL: https://linkinghub.elsevier. com/retrieve/pii/S0950061820310072.
- Du, Y., Yang, W., Ge, Y., Wang, S., Liu, P., 2021. Thermal conductivity of cement paste containing waste glass powder, metakaolin and limestone filler as supplementary cementitious material. J. Clean. Prod. 287, 125018 https://doi.org/10.1016/j. jclepro.2020.125018. URL: https://linkinghub.elsevier.com/retrieve/pii/S0959652 620350629.
- Heriyanto, F. Pahlevani, Sahajwalla, V., 2018. From waste glass to building materials an innovative sustainable solution for waste glass. J. Clean. Prod. 191, 192–206. https://doi.org/10.1016/j.jclepro.2018.04.214. URL: https://linkinghub.elsevier.com/retrieve/pii/S0959652618312502.
- Hossain, M.U., Ng, S.T., Antwi-Afari, P., Amor, B., 2020. Circular economy and the construction industry: existing trends, challenges and prospective framework for sustainable construction. Renew. Sustain. Energy Rev. 130, 109948 https://doi.org/ 10.1016/j.rser.2020.109948. URL: https://linkinghub.elsevier.com/retrieve/pii (\$136.402313023232)
- Huynh, T.-P., Vo, D.-H., Hwang, C.-L., 2018. Engineering and durability properties of eco-friendly mortar using cement-free srf binder. Construct. Build. Mater. 160, 145–155. https://doi.org/10.1016/j.conbuildmat.2017.11.040. URL: https://linkinghub.elsevier.com/retrieve/pii/S0950061817322511.
- Kim, J., Yi, C., Zi, G., 2015. Waste glass sludge as a partial cement replacement in mortar. Construct. Build. Mater. 75, 242–246. https://doi.org/10.1016/j. conbuildmat.2014.11.007. URL: https://linkinghub.elsevier.com/retrieve/pii/S0950061814012197.
- Kyklos, 2020. Estudio del Material Disponible País (MDP) y el reciclado de los Envases y Embalajes de Vidrio en Chile. ANIR, Santiago. URL: https://www.anir.cl/wp-co ntent/uploads/2021/12/ANIR-2020-Estudio-del-material-disponible-Pais-Vidrio. ndf
- Letelier, V., Henríquez-Jara, B.I., Manosalva, M., Parodi, C., Ortega, J.M., 2019a. Use of waste glass as a replacement for raw materials in mortars with a lower environmental impact. Energies 12, 1974. https://doi.org/10.3390/en12101974. URL: https://www.mdpi.com/1996-1073/12/10/1974.
- Letelier, V., Henríquez-Jara, B.I., Manosalva, M., Moriconi, G., 2019b. Combined use of waste concrete and glass as a replacement for mortar raw materials. Waste Manag. 94, 107–119. https://doi.org/10.1016/j.wasman.2019.05.041. URL: https://linkinghub.elsevier.com/retrieve/pii/S0956053X19303496.
- Letelier, V., Bustamante, M., Muñoz, P., Rivas, S., Ortega, J.M., 2021. Evaluation of mortars with combined use of fine recycled aggregates and waste crumb rubber. J. Build. Eng. 43, 103226 https://doi.org/10.1016/j.jobe.2021.103226. URL: htt ps://linkinghub.elsevier.com/retrieve/pii/S2352710221010846.
- Marie, I., 2017. Thermal conductivity of hybrid recycled aggregate rubberized concrete. Construct. Build. Mater. 133, 516–524. https://doi.org/10.1016/j.conbuildmat.2016.12.113. URL: https://linkinghub.elsevier.com/retrieve/pii/S0050061816320335
- Mejdi, M., Wilson, W., Saillio, M., Chaussadent, T., Divet, L., Tagnit-Hamou, A., 2022. Hydration and microstructure of glass powder cement pastes – a multi-technique investigation. Cement Concr. Res. 151, 106610 https://doi.org/10.1016/j. cemconres.2021.106610. URL: https://linkinghub.elsevier.com/retrieve/pii /S0008884621002593.
- Moreno, D.D.P., Ribeiro, S., Saron, C., 2020. Compatibilization of Recycled Rubber Aggregate in Mortar, Materials and Structures, vol. 53, p. 23. https://doi.org/

- 10.1617/s11527-020-1456-4. **URL:** http://link.springer.com/10.1617/s11527-020-1456-4
- Mundo, R.D., Seara-Paz, S., González-Fonteboa, B., Notarnicola, M., 2020. Masonry and render mortars with tyre rubber as aggregate: fresh state rheology and hardened state performances. Construct. Build. Mater. 245, 118359 https://doi.org/10.1016/j. conbuildmat.2020.118359. URL: https://linkinghub.elsevier.com/retrieve/pii /S0950061820303640
- Nahi, S., Leklou, N., Khelidj, A., Oudjit, M.N., Zenati, A., 2020. Properties of cement pastes and mortars containing recycled green glass powder. Construct. Build. Mater. 262, 120875 https://doi.org/10.1016/j.conbuildmat.2020.120875. URL: https://linkinghub.elsevier.com/retrieve/pii/S0950061820328804.
- NCh2256/1.Of2001, 2001. Morteros Parte 1: Requisitos Generales. INN, Santiago.
- Norambuena-Contreras, J., Quilodran, J., Gonzalez-Torre, I., Chavez, M., Borinaga-Treviño, R., 2018. Electrical and thermal characterisation of cement-based mortars containing recycled metallic waste. J. Clean. Prod. 190, 737–751. https://doi.org/10.1016/j.jclepro.2018.04.176. URL: https://linkinghub.elsevier.com/retrieve/pii/S0959652618312095
- OECD, 2019. Global Material Resources Outlook to 2060: Economic Drivers and Environmental Consequences. OECD Publishing. https://doi.org/10.1787/ 9789264307452-en
- Ortega, J., Letelier, V., Solas, C., Miró, M., Moriconi, G., Climent, M., Sánchez, I., 2018. Influence of waste glass powder addition on the pore structure and service properties of cement mortars. Sustainability 10, 842. https://doi.org/10.3390/su10030842. URL: http://www.mdpi.com/2071-1050/10/3/842.
- Ramdani, S., Guettala, A., Benmalek, M., Aguiar, J.B., 2019. Physical and mechanical performance of concrete made with waste rubber aggregate, glass powder and silica sand powder. J. Build. Eng. 21, 302–311. https://doi.org/10.1016/j. jobe.2018.11.003. URL: https://linkinghub.elsevier.com/retrieve/pii/S2352710 218307174
- Ren, F., Mo, J., Wang, Q., Ho, J.C.M., 2022. Crumb rubber as partial replacement for fine aggregate in concrete: an overview. Construct. Build. Mater. 343, 128049 https:// doi.org/10.1016/j.conbuildmat.2022.128049. URL: https://linkinghub.elsevier. com/retrieve/pii/S0950061822017160.
- UNE-EN 1015-10, 2000. Methods of Test for Mortar for Masonry Part 10: Determination of Dry Bulk Density of Hardened Mortar. AENOR, Madrid.
- UNE-EN 1015-18, 2003. Methods of Test for Mortar for Masonry Part 18: Determination of Water Absorption Coefficient Due to Capillary Action of Hardened Mortar. AENOR, Madrid.
- UNE-EN 196-1, 1996. Methods of Testing Cement Part 1: Determination of Strength. AENOR, Madrid.
- Wang, J., Guo, Z., Yuan, Q., Zhang, P., Fang, H., 2020. Effects of ages on the itz microstructure of crumb rubber concrete. Construct. Build. Mater. 254, 119329 https://doi.org/10.1016/j.conbuildmat.2020.119329. URL: https://linkinghub.else vier.com/retrieve/pii/S0950061820313349.
- xin Lu, J., hua Duan, Z., Poon, C.S., 2017. Combined use of waste glass powder and cullet in architectural mortar. Cement Concr. Compos. 82, 34–44. https://doi.org/ 10.1016/j.cemconcomp.2017.05.011. URL: https://linkinghub.elsevier.com/retrie/ ve/ni//S095894651630395X
- Xu, J., Yao, Z., Yang, G., Han, Q., 2020. Research on crumb rubber concrete: from a multi-scale review. Construct. Build. Mater. 232, 117282 https://doi.org/10.1016/j. conbuildmat.2019.117282. URL: https://linkinghub.elsevier.com/retrieve/pii /S0950061819327345.
- Youssf, O., ElGawady, M.A., Mills, J.E., 2015. Experimental investigation of crumb rubber concrete columns under seismic loading. Structures 3, 13–27. https://doi. org/10.1016/j.istruc.2015.02.005. URL: https://linkinghub.elsevier.com/retrieve/pii/S2352012415000326.
- Zhu, Q., Dai, H., Chen, D., Liang, Z., 2019. Study on influence of waste tire rubber particles on concrete crack resistance at early age. IOP Conf. Ser. Earth Environ. Sci. 242, 052060 https://doi.org/10.1088/1755-1315/242/5/052060. URL: https://iopscience.iop.org/article/10.1088/1755-1315/242/5/052060.